Composite Structures 337 (2024) 118078

Contents lists available at ScienceDirect

Composite Structures

journal homepage: www.elsevier.com/locate/compstruct

Closed-form solutions for axially non-uniform Timoshenko beams and frames under static loading

Juan Camilo Molina-Villegas [a,*], Jorge Eliecer Ballesteros Ortega [b], Simón Benítez Soto [a]

[a] Escuela de Ciencias Aplicadas e Ingeniería, Universidad EAFIT, Medellín, Colombia
[b] Department of Civil, Environmental, and Construction Engineering, University of Central Florida, Orlando, FL 32816, USA

ARTICLE INFO

Keywords:
Axially non-uniform Timoshenko beams
Closed-form solution
Green's functions
Finite element method
Mesh reduction method
Framed structures
Composite materials

ABSTRACT

This paper presents the Green's Functions Stiffness Method (GFSM) for solving linear elastic static problems in arbitrary axially non-uniform Timoshenko beams and frames subjected to general external loads and bending moments. The GFSM is a mesh reduction method that seamlessly integrates elements from the Stiffness Method (SM), Finite Element Method (FEM), and Green's Functions (GFs), resulting in a highly versatile methodology for structural analysis. It incorporates fundamental concepts such as stiffness matrices, shape functions, and fixed-end forces, in line with SM and FEM frameworks. Leveraging the capabilities of GFs, the method facilitates the derivation of closed-form solutions, addressing a gap in existing methods for analyzing non-uniform reticular structures which are typically limited to simple cases like single-span beams with specific axial variations and loading scenarios. The effectiveness of the GFSM is demonstrated through three practical examples, showcasing its applicability in analyzing non-uniform beams and plane frames, thereby broadening the scope of closed-form solutions for axially non-uniform Timoshenko structures.

1. Introduction

The stress and strain fields experienced by structural elements exhibit spatial variability, diminishing the effectiveness of uniform elements from a mechanical perspective, as their strength and stiffness distribution do not adapt to those changing conditions. Non-uniform structural elements, characterized by variations in cross-section and material, are extensively employed to address these changing conditions, offering optimization in strength and stiffness, and in weight reduction [1,2]. In aerospace engineering, non-uniform elements find application in wing and blade structures subjected to aerodynamic loads. Similarly, in structural engineering, they are utilized in buildings to accommodate varying internal forces distributions and architectural requirements. In mechanical engineering, non-uniform elements are employed in machine components such as shafts, and gears.

Among heterogeneous materials, Functionally Graded Materials (FGMs) are notable for their gradual mechanical property changes [3–5]. FGMs, as second-generation composites, are highly versatile for applications in biomedical, aerospace, naval, mechanical, and civil structures [6,7]. When mechanical properties vary exclusively along the axial direction, they are classified as Axially Functionally Graded (AFG) materials [8], while axially non-uniform elements encompass both non-uniform cross-sections and AFGMs.

Due to the kinematic model used to describe them, non-uniform elements of reticular structures are commonly idealized using beam [9] or the plane stress models [10,11]. In particular, the Euler–Bernoulli and Timoshenko beam models are the most widely used, being the main difference between them that in the Timoshenko theory the plane cross-section of the beam remains plane after the external loads are applied but can rotate with respect to the beam centroidal-line, while in the Euler–Bernoulli theory, the cross-section is always perpendicular to that line [12].

In recent decades, various methods have been employed to analyze axially non-uniform static Euler–Bernoulli and Timoshenko beams and frames. The Finite Element Method (FEM) has been widely used, providing stiffness matrices and fixed-end forces for common axially non-uniform elements and arbitrary non-uniform elements [13–20]. Alternative methods have also been explored, including the use of generalized functions [21], Laplace transform [22], and the transformation of Differential Equations (DEs) of variable coefficients into DE of constant coefficients [23,24]. Additionally, exact elastic solutions for FGMs have been presented [25,26]. For Timoshenko beams, FEM has been prevalent, offering various solutions ranging from simple to complex models, with alternative approaches proposed by other researchers [27–35].

* Corresponding author.
E-mail address: jmolina2@eafit.edu.co (J.C. Molina-Villegas).

https://doi.org/10.1016/j.compstruct.2024.118078
Received 17 October 2023; Received in revised form 13 February 2024; Accepted 21 March 2024
Available online 23 March 2024

Numerous efforts have been undertaken to investigate the dynamic response of non-uniform beams and frames, both in the time and frequency domains. For the Euler–Bernoulli model, Gupta [36] computed the stiffness and consistent mass matrices for linearly tapered beams, while Banerjee [37] calculated the dynamic stiffness matrix. Additionally, the free vibrations of such beams have been extensively studied [38–41]. The response of these beams on elastic foundation has also been explored [42]. In the case of the Timoshenko beam model, its free vibration has been analyzed by [43], with an approximated model proposed in [44], and an asymptotic model suggested in [45].

The Green's Functions Stiffness Method (GFSM) presents an alternative approach for analyzing arbitrarily axially non-uniform beams and frames, as demonstrated in [46] for Euler–Bernoulli beams and frames. This is a novel mesh reduction method closely related to the FEM and the Stiffness Method (SM), sharing with those the use of shape functions, stiffness matrices, and fixed-end forces; all of them being exact in the case of the GFSM. This makes its matrix formulation equal to the Transcendental Finite Element Method (TFEM) [47,48], with the key differentiator of the GFSM lying in the utilization of Green's Functions (GFs) of fixed elements. This characteristic enables the derivation of closed-form solutions for reticular structures subjected to arbitrary loads and moments.

The effectiveness of the GFSM has been demonstrated across various scenarios, including static analysis of Euler–Bernoulli beams and frames [49], beams on elastic Winkler foundations [50,51], static Timoshenko beams and frames [52,53]; as well as the dynamic analysis of Euler–Bernoulli beams and frames [54,55]. These applications highlight its efficiency and versatility in structural analysis.

While numerous methods have been developed, there exists a gap in the literature concerning a readily implementable approach to derive closed-form solutions for statically linearly elastic arbitrary axially non-uniform Timoshenko beams and frames subjected to general external loads and bending moments. To address this gap, this paper presents the formulation of the GFSM for analyzing these structures.

The paper is structured into seven sections. Section 2 introduces the decomposition of the axially non-uniform Timoshenko frame element into axially non-uniform Timoshenko beam and rod elements. The formulation for these individual elements is presented in Sections 3 and 4, respectively. In Section 5, the beam and rod formulations are merged to present the GFSM for the axially non-uniform Timoshenko frame element. Section 6 illustrates its applicability through three examples, two for beams and another for a plane frame structure. Finally, Section 7 summarizes the conclusions.

2. Decomposition of the Timoshenko frame element

The element to be studied is the axially non-uniform Timoshenko frame element presented in Fig. 1. It has an axially non-uniform linear elastic material with Young's modulus $E(x)$, and shear modulus $G(x)$, a variable cross-section with area $A(x)$, shear coefficient $\kappa(x)$ [56], shear area $A_s(x) = \kappa(x)A(x)$, and second moment of area about the z-axis $I(x)$. The element is subjected to arbitrary external distributed axial load $p(x)$, transverse distributed load $q_v(x)$, and distributed bending moment $q_\theta(x)$.

The internal forces fields of the element include the axial force $P(x)$, the shear force $V(x)$, and the bending moment about the z-axis $M(x)$, all of which follow the positive sign convention depicted in Fig. 2.

Utilizing a first-order theory, the transverse and axial behaviors of the axially non-uniform Timoshenko frame element are decoupled. This enables its decomposition into an axially non-uniform Timoshenko beam element (Fig. 3(a)) and an axially non-uniform rod element (Fig. 3(b)).

3. Formulation of the GFSM for the axially non-uniform timoshenko beam element

3.1. Governing boundary value problem

The internal forces in the axially non-uniform Timoshenko beam element are caused by its deformation, expressed in terms of the displacement and cross-section rotation fields as [57]:

$$M(x) = EI(x)\frac{\mathrm{d}\theta}{\mathrm{d}x}(x) \tag{1a}$$

$$V(x) = A_sG(x)\left[\frac{\mathrm{d}v}{\mathrm{d}x}(x) - \theta(x)\right] \tag{1b}$$

where $EI(x) = E(x)I(x)$ and $A_sG(x) = A_s(x)G(x)$ are the element flexural and shear rigidities, $v(x)$ is the transverse displacement field (positive in the y-axis direction), and $\theta(x)$ is the cross-section rotation field (positive about the z-axis direction, i.e., counter clockwise).

The vertical and rotational differential equilibrium equations for any beam element are:

$$\frac{\mathrm{d}V}{\mathrm{d}x}(x) = -q_v(x) \tag{2a}$$

$$\frac{\mathrm{d}M}{\mathrm{d}x}(x) + V(x) = -q_\theta(x) \tag{2b}$$

Substituting Eqs. (1) into Eqs. (2), the coupled governing Differential Equations (DEs) for the axially non-uniform Timoshenko beam element are obtained [35]:

$$\frac{\mathrm{d}}{\mathrm{d}x}\left\{A_sG(x)\left[\frac{\mathrm{d}v}{\mathrm{d}x}(x) - \theta(x)\right]\right\} = -q_v(x) \tag{3a}$$

$$\frac{\mathrm{d}}{\mathrm{d}x}\left[EI(x)\frac{\mathrm{d}\theta}{\mathrm{d}x}(x)\right] + A_sG(x)\left[\frac{\mathrm{d}v}{\mathrm{d}x}(x) - \theta(x)\right] = -q_\theta(x) \tag{3b}$$

It is important to mention that an alternative to the coupled DEs (3) is to combine those in a single fourth order differential equation with variable coefficients as proposed in [58]. Because the GFSM is based on a strong formulation, four Boundary Conditions (BCs) should be added to the DEs (3), being the governing Boundary Value Problem (BVP) defined as:

$$\frac{\mathrm{d}}{\mathrm{d}x}\left\{A_sG(x)\left[\frac{\mathrm{d}v}{\mathrm{d}x}(x) - \theta(x)\right]\right\} = -q_v(x) \tag{4a}$$

$$\frac{\mathrm{d}}{\mathrm{d}x}\left[EI(x)\frac{\mathrm{d}\theta}{\mathrm{d}x}(x)\right] + A_sG(x)\left[\frac{\mathrm{d}v}{\mathrm{d}x}(x) - \theta(x)\right] = -q_\theta(x) \tag{4b}$$

$$v(0) = v_i \tag{4c}$$

$$\theta(0) = \theta_i \tag{4d}$$

$$v(L) = v_j \tag{4e}$$

$$\theta(L) = \theta_j \tag{4f}$$

where v_i and v_j are the y-axis displacement at $x = 0$ and $x = L$ respectively, whereas θ_i and θ_j are the rotations of the cross-section at the same points.

To help solve the BVP presented in Eqs. (4), its solution is decomposed into a homogeneous (denoted using the subscript h) and a particular or "fixed" (denoted using the subscript f) solutions (see Fig. 4). The transverse displacement, cross-section rotation, bending moment, and shear force fields are defined, respectively, as:

$$v(x) = v_h(x) + v_f(x) \tag{5a}$$

$$\theta(x) = \theta_h(x) + \theta_f(x) \tag{5b}$$

$$M(x) = M_h(x) + M_f(x) \tag{5c}$$

$$V(x) = V_h(x) + V_f(x) \tag{5d}$$

In Sections 3.2 and 3.3, the solutions of the homogeneous and fixed responses are presented.

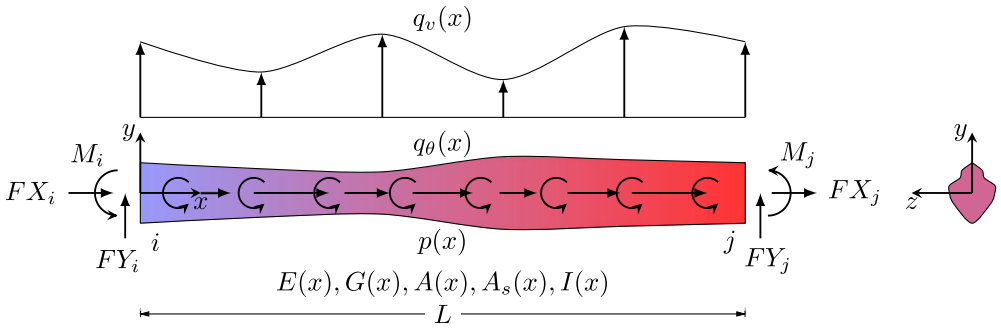

Fig. 1. Axially non-uniform Timoshenko frame element.

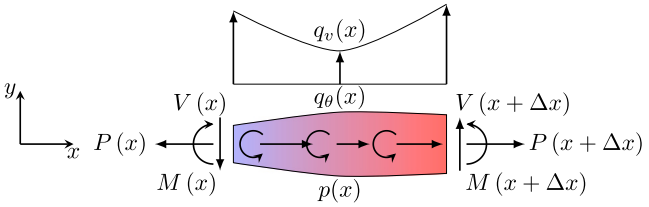

Fig. 2. Internal forces positive sign convention.

3.2. Homogeneous response

The governing BVP for the homogeneous response of the axially non-uniform Timoshenko beam element is (see Fig. 4(a)):

$$\frac{\mathrm{d}}{\mathrm{d}x}\left\{A_sG(x)\left[\frac{\mathrm{d}v_h}{\mathrm{d}x}(x)-\theta_h(x)\right]\right\}=0 \tag{6a}$$

$$\frac{\mathrm{d}}{\mathrm{d}x}\left[EI(x)\frac{\mathrm{d}\theta_h}{\mathrm{d}x}(x)\right]+A_sG(x)\left[\frac{\mathrm{d}v_h}{\mathrm{d}x}(x)-\theta(x)\right]=0 \tag{6b}$$

$$v_h(0)=v_i \tag{6c}$$

$$\theta_h(0)=\theta_i \tag{6d}$$

$$v_h(L)=v_j \tag{6e}$$

$$\theta_h(L)=\theta_j \tag{6f}$$

An easy way to solve the BVP (6) is to start integrating both sides of Eq. (6a) to obtain:

$$V_h(x)=A_sG(x)\left[\frac{\mathrm{d}v_h}{\mathrm{d}x}(x)-\theta_h(x)\right]=C_1 \tag{7}$$

By substituting Eq. (7) into Eq. (6b) and solving the resulting equation for $\theta_h(x)$, gets as result:

$$\theta_h(x)=-C_1\int_0^x\frac{s}{EI(s)}\mathrm{d}s+C_2\int_0^x\frac{1}{EI(s)}\mathrm{d}s+\theta_i \tag{8}$$

where the Boundary Condition (BC) (6d) was used.

Substituting Eq. (8) into Eq. (7) and solving for $v_h(x)$, yield:

$$v_h(x)=C_1\int_0^x\frac{1}{A_sG(\chi)}\mathrm{d}\chi-C_1\int_0^x\left[\int_0^\chi\frac{s}{EI(s)}\mathrm{d}s\right]\mathrm{d}\chi + C_2\int_0^x\left[\int_0^\chi\frac{1}{EI(s)}\mathrm{d}s\right]\mathrm{d}\chi+\theta_i x+v_i \tag{9}$$

Where the BC (6c) was employed.

Evaluating Eqs. (8) and (9) at $x=L$ and applying the boundary conditions (6e) and (6f) yield the following system of two linear equations:

$$\theta_j=-C_1\cdot\mathcal{I}_3(L)+C_2\cdot\mathcal{I}_4(L)+\theta_i \tag{10a}$$

$$v_j=C_1\cdot\mathcal{I}_5(L)-C_1\cdot\mathcal{I}_1(L)+C_2\cdot\mathcal{I}_2(L)+\theta_iL+v_i \tag{10b}$$

where

$$\mathcal{I}_1(x)=\int_0^x\left[\int_0^\chi\frac{s}{EI(s)}\mathrm{d}s\right]\mathrm{d}\chi=\int_0^x\mathcal{I}_3(\chi)\mathrm{d}\chi \tag{11a}$$

$$\mathcal{I}_2(x)=\int_0^x\left[\int_0^\chi\frac{1}{EI(s)}\mathrm{d}s\right]\mathrm{d}\chi=\int_0^x\mathcal{I}_4(\chi)\mathrm{d}\chi \tag{11b}$$

$$\mathcal{I}_3(x)=\int_0^x\frac{s}{EI(s)}\mathrm{d}s \tag{11c}$$

$$\mathcal{I}_4(x)=\int_0^x\frac{1}{EI(s)}\mathrm{d}s \tag{11d}$$

$$\mathcal{I}_5(x)=\int_0^x\frac{1}{A_sG(s)}\mathrm{d}s \tag{11e}$$

From the solution of Eqs. (10), the values of C_1 and C_2 are obtained:

$$C_1=\frac{\mathcal{I}_4(L)\cdot v_i+\left[\mathcal{I}_4(L)\cdot L-\mathcal{I}_2(L)\right]\theta_i-\mathcal{I}_4(L)\cdot v_j+\mathcal{I}_2(L)\cdot\theta_j}{D} \tag{12a}$$

$$C_2=\frac{\mathcal{I}_3(L)\cdot v_i+\left[-\mathcal{I}_1(L)+\mathcal{I}_5(L)+\mathcal{I}_3(L)\cdot L\right]\theta_i-\mathcal{I}_3(L)\cdot v_j+\left[\mathcal{I}_1(L)-\mathcal{I}_5(L)\right]\theta_j}{D} \tag{12b}$$

being

$$D=\left[\mathcal{I}_1(L)-\mathcal{I}_5(L)\right]\cdot\mathcal{I}_4(L)-\mathcal{I}_2(L)\cdot\mathcal{I}_3(L) \tag{13}$$

By substituting Eqs. (12) into Eqs. (8) and (9), the following equations are obtained:

$$v_h(x)=\psi_2^v(x)v_i+\psi_3^v(x)\theta_i+\psi_5^v(x)v_j+\psi_6^v(x)\theta_j \tag{14a}$$

$$\theta_h(x)=\psi_2^\theta(x)v_i+\psi_3^\theta(x)\theta_i+\psi_5^\theta(x)v_j+\psi_6^\theta(x)\theta_j \tag{14b}$$

where

$$\psi_2^v(x)=-\frac{\mathcal{I}_4(L)}{D}[\mathcal{I}_1(x)-\mathcal{I}_5(x)]+\frac{\mathcal{I}_3(L)}{D}\mathcal{I}_2(x)+1 \tag{15a}$$

$$\psi_3^v(x)=-\frac{\mathcal{I}_3(L)}{D}[\mathcal{I}_1(x)-\mathcal{I}_5(x)]+\frac{-\mathcal{I}_1(L)+\mathcal{I}_5(L)+\mathcal{I}_3(L)\cdot L}{D}\mathcal{I}_2(x)+x \tag{15b}$$

$$\psi_5^v(x)=\frac{\mathcal{I}_4(L)}{D}[\mathcal{I}_1(x)-\mathcal{I}_5(x)]-\frac{\mathcal{I}_3(L)}{D}\mathcal{I}_2(x) \tag{15c}$$

$$\psi_6^v(x)=-\frac{\mathcal{I}_2(L)}{D}[\mathcal{I}_1(x)-\mathcal{I}_5(x)]+\frac{\mathcal{I}_1(L)-\mathcal{I}_5(L)}{D}\mathcal{I}_2(x) \tag{15d}$$

and

$$\psi_2^\theta(x)=-\frac{\mathcal{I}_4(L)}{D}\mathcal{I}_3(x)+\frac{\mathcal{I}_3(L)}{D}\mathcal{I}_4(x) \tag{16a}$$

$$\psi_3^\theta(x)=-\frac{\mathcal{I}_3(L)}{D}\mathcal{I}_3(x)+\frac{-\mathcal{I}_1(L)+\mathcal{I}_5(L)+\mathcal{I}_3(L)\cdot L}{D}\mathcal{I}_4(x)+1 \tag{16b}$$

$$\psi_5^\theta(x)=\frac{\mathcal{I}_4(L)}{D}\mathcal{I}_3(x)-\frac{\mathcal{I}_3(L)}{D}\mathcal{I}_4(x) \tag{16c}$$

$$\psi_6^\theta(x)=-\frac{\mathcal{I}_2(L)}{D}\mathcal{I}_3(x)+\frac{\mathcal{I}_1(L)-\mathcal{I}_5(L)}{D}\mathcal{I}_4(x) \tag{16d}$$

The functions $\psi_n^v(x)$ and $\psi_n^\theta(x)$ $(n=2,3,5,6)$ are the analytical displacement and rotation shape functions for the axially non-uniform Timoshenko beam element, respectively, being the same used in the TFEM [59].

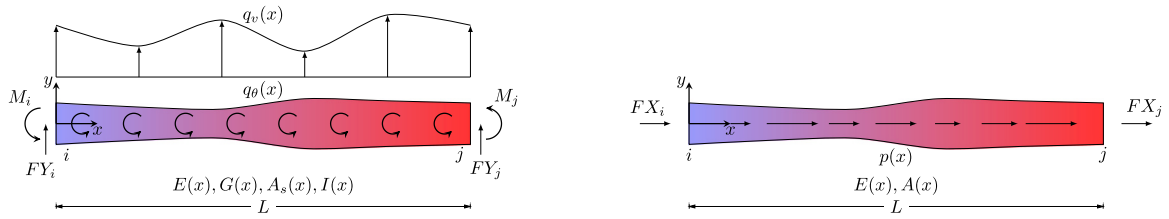

(a) Axially non-uniform Timoshenko beam element. (b) Axially non-uniform rod element.

Fig. 3. Decomposition of the axially non-uniform Timoshenko frame element as an axially non-uniform Timoshenko beam and axially non-uniform rod elements.

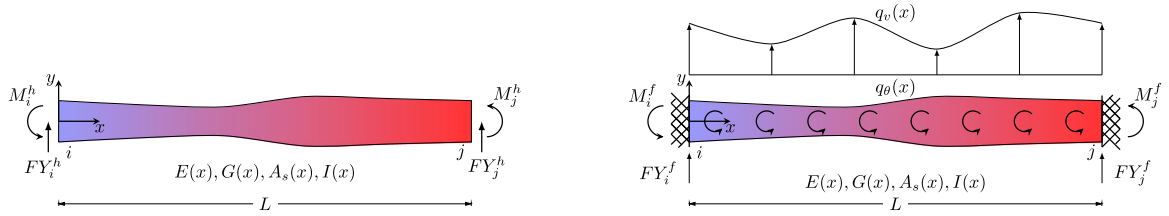

(a) Homogeneous response. (b) Fixed response.

Fig. 4. Decomposition of the response of axially non-uniform Timoshenko beam element.

Using Eqs. (1), the homogeneous internal forces fields can be readily computed from the homogeneous transverse displacement and cross-section rotation fields presented in Eqs. (15) and (16) respectively, resulting in:

$$M_h(x) = \psi_2^M(x)v_i + \psi_3^M(x)\theta_i + \psi_5^M(x)v_j + \psi_6^M(x)\theta_j \tag{17a}$$

$$V_h(x) = \psi_2^V(x)v_i + \psi_3^V(x)\theta_i + \psi_5^V(x)v_j + \psi_6^V(x)\theta_j \tag{17b}$$

where

$$\psi_2^M(x) = \frac{\mathcal{I}_3(L)}{D} - \frac{\mathcal{I}_4(L)}{D}x \tag{18a}$$

$$\psi_3^M(x) = \frac{-\mathcal{I}_1(L) + \mathcal{I}_5(L) + \mathcal{I}_3(L)\cdot L}{D} - \frac{\mathcal{I}_3(L)}{D}x \tag{18b}$$

$$\psi_5^M(x) = -\frac{\mathcal{I}_3(L)}{D} + \frac{\mathcal{I}_4(L)}{D}x \tag{18c}$$

$$\psi_6^M(x) = \frac{\mathcal{I}_1(L) - \mathcal{I}_5(L)}{D} - \frac{\mathcal{I}_2(L)}{D}x \tag{18d}$$

and

$$\psi_2^V(x) = \frac{\mathcal{I}_4(L)}{D} \tag{19a}$$

$$\psi_3^V(x) = \frac{\mathcal{I}_3(L)}{D} \tag{19b}$$

$$\psi_5^V(x) = -\frac{\mathcal{I}_4(L)}{D} \tag{19c}$$

$$\psi_6^V(x) = \frac{\mathcal{I}_2(L)}{D} \tag{19d}$$

being the functions $\psi_n^M(x)$ and $\psi_n^V(x)$ $(n = 2,3,5,6)$ defined as the bending moment and shear force shape functions, respectively.

From the evaluation of the homogeneous internal force fields at $x = 0$ and $x = L$, the relation between the generalized forces and displacements at the ends of the element are obtained (compare Fig. 2 with Fig. 4(a) to see the difference between the positive sign conventions for the internal forces and the forces at the ends of the elements):

$$\begin{Bmatrix} FY_i^h \\ M_i^h \\ FY_j^h \\ M_j^h \end{Bmatrix} = \begin{Bmatrix} -V_h(0) \\ -M_h(0) \\ V_h(L) \\ M_h(L) \end{Bmatrix} = \begin{bmatrix} k_{22} & k_{23} & k_{25} & k_{26} \\ k_{32} & k_{33} & k_{35} & k_{36} \\ k_{52} & k_{53} & k_{55} & k_{56} \\ k_{62} & k_{63} & k_{65} & k_{66} \end{bmatrix} \begin{Bmatrix} v_i \\ \theta_i \\ v_j \\ \theta_j \end{Bmatrix} \tag{20}$$

being

$$k_{22} = k_{55} = -k_{25} = -k_{52} = -\frac{\mathcal{I}_4(L)}{D} \tag{21a}$$

$$k_{23} = k_{32} = -k_{35} = -k_{53} = -\frac{\mathcal{I}_3(L)}{D} \tag{21b}$$

$$k_{26} = k_{62} = -k_{56} = -k_{65} = -\frac{\mathcal{I}_2(L)}{D} \tag{21c}$$

$$k_{33} = \frac{\mathcal{I}_1(L) - \mathcal{I}_5(L) - \mathcal{I}_3(L)\cdot L}{D} \tag{21d}$$

$$k_{36} = k_{63} = -\frac{\mathcal{I}_1(L) - \mathcal{I}_5(L)}{D} \tag{21e}$$

$$k_{66} = \frac{\mathcal{I}_1(L) - \mathcal{I}_5(L) - \mathcal{I}_2(L)\cdot L}{D} \tag{21f}$$

where the following identity has been used:

$$\mathcal{I}_2(x) + \mathcal{I}_3(x) = \mathcal{I}_4(x)\cdot x \tag{22}$$

The 4×4 matrix presented in Eq. (20) is the analytic stiffness matrix for the axially non-uniform Timoshenko beam element, which is equivalent the one used in the TFEM [16,19,28].

3.3. Fixed response

The governing BVP for the fixed response of the axially non-uniform Timoshenko beam element is (see Fig. 4(b)):

$$\frac{\mathrm{d}}{\mathrm{d}x}\left\{A_s G(x)\left[\frac{\mathrm{d}v_f}{\mathrm{d}x}(x) - \theta_f(x)\right]\right\} = -q_v(x) \tag{23a}$$

$$\frac{\mathrm{d}}{\mathrm{d}x}\left[EI(x)\frac{\mathrm{d}\theta_f}{\mathrm{d}x}(x)\right] + A_s G(x)\left[\frac{\mathrm{d}v_f}{\mathrm{d}x}(x) - \theta_f(x)\right] = -q_\theta(x) \tag{23b}$$

$$v_f(0) = 0 \tag{23c}$$

$$\theta_f(0) = 0 \tag{23d}$$

$$v_f(L) = 0 \tag{23e}$$

$$\theta_f(L) = 0 \tag{23f}$$

To solve the BVP (23) the fixed response will be decomposed into two parts, one caused by the arbitrary external load $q_v(x)$ (denoted using the superscript v), and the other part caused by the arbitrary external moments $q_\theta(x)$ (denoted using the superscript θ) as presented

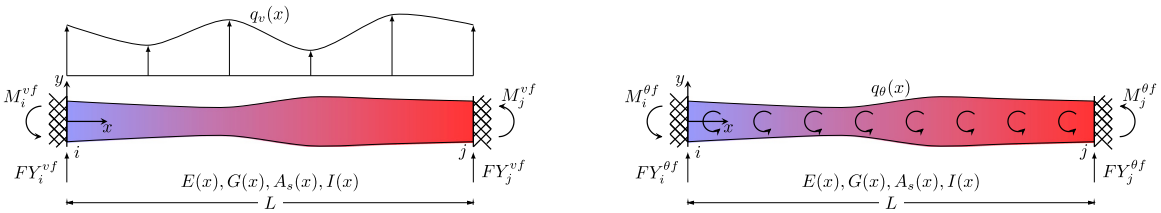

(a) Fixed response due to the external transverse load $q_v(x)$.

(b) Fixed response due to the external bending moment $q_\theta(x)$.

Fig. 5. Decomposition of the fixed response of the axially non-uniform Timoshenko beam element.

in Fig. 5. Being the transverse displacement, cross-section rotation, bending moment, and shear force fixed fields defined respectively, as:

$$v_f(x) = v_f^v(x) + v_f^\theta(x) \tag{24a}$$
$$\theta_f(x) = \theta_f^v(x) + \theta_f^\theta(x) \tag{24b}$$
$$M_f(x) = M_f^v(x) + M_f^\theta(x) \tag{24c}$$
$$V_f(x) = V_f^v(x) + V_f^\theta(x) \tag{24d}$$

3.3.1. Fixed response due to $q_v(x)$

The displacement Green's function $G_{yy}(x,\xi)$ associated with the studied element is defined as the transverse displacement field when it is fixed and subjected to a point unit transverse external load at ξ (see Fig. 6). This function has two intervals and is defined as follows:

$$G_{yy}(x,\xi) = \begin{cases} G_{yy}^I(x,\xi) & 0 < x \le \xi \\ G_{yy}^{II}(x,\xi) & \xi \le x < L \end{cases} \tag{25}$$

being

$$G_{yy}^I(x,\xi) = W_2^v(x)\psi_2^v(\xi) + W_3^v(x)\psi_3^v(\xi) \tag{26a}$$
$$G_{yy}^{II}(x,\xi) = W_5^v(x)\psi_5^v(\xi) + W_6^v(x)\psi_6^v(\xi) \tag{26b}$$

where

$$W_2^v(x) = -\mathcal{I}_1(x) + \mathcal{I}_5(x) \tag{27a}$$
$$W_3^v(x) = \mathcal{I}_2(x) \tag{27b}$$
$$W_5^v(x) = -\mathcal{I}_1(L) + \mathcal{I}_5(L) + x\cdot\mathcal{I}_2(L) + \mathcal{I}_1(x) - \mathcal{I}_5(x) - L\cdot\mathcal{I}_2(x) \tag{27c}$$
$$W_6^v(x) = x\cdot\left[\mathcal{I}_4(L) - \mathcal{I}_4(x)\right] - \left[\mathcal{I}_3(L) - \mathcal{I}_3(x)\right] \tag{27d}$$

The cross-section rotation field associated with the displacement Green's function $G_{yy}(x,\xi)$ is called the rotation Green's function, which is expressed as $G_{\theta y}(x,\xi)$, established as:

$$G_{\theta y}^I(x,\xi) = W_2^\theta(x)\psi_2^v(\xi) + W_3^\theta(x)\psi_3^v(\xi) \tag{28a}$$
$$G_{\theta y}^{II}(x,\xi) = W_5^\theta(x)\psi_5^v(\xi) + W_6^\theta(x)\psi_6^v(\xi) \tag{28b}$$

being

$$W_2^\theta(x) = -\mathcal{I}_3(x) \tag{29a}$$
$$W_3^\theta(x) = \mathcal{I}_4(x) \tag{29b}$$
$$W_5^\theta(x) = \mathcal{I}_2(L) - \mathcal{I}_2(x) - (L-x)\cdot\mathcal{I}_4(x) \tag{29c}$$
$$W_6^\theta(x) = \mathcal{I}_4(L) - \mathcal{I}_4(x) \tag{29d}$$

Following [46], the fixed displacement field $v_f^v(x)$ and the fixed cross-section rotation field $\theta_f^v(x)$ caused by the external load $q_v(x)$ are computed as follows:

$$v_f^v(x) = \int_0^x G_{yy}^{II}(x,\xi)q_v(\xi)\mathrm{d}\xi + \int_x^L G_{yy}^I(x,\xi)q_v(\xi)\mathrm{d}\xi \tag{30a}$$
$$\theta_f^v(x) = \int_0^x G_{\theta y}^{II}(x,\xi)q_v(\xi)\mathrm{d}\xi + \int_x^L G_{\theta y}^I(x,\xi)q_v(\xi)\mathrm{d}\xi \tag{30b}$$

Substituting Eqs. (30) into Eqs. (1), the bending moment and shear force fields are obtained:

$$M_f^v(x) = \int_0^x G_{M_y}^{II}(x,\xi)q_v(\xi)\mathrm{d}\xi + \int_x^L G_{M_y}^I(x,\xi)q_v(\xi)\mathrm{d}\xi \tag{31a}$$
$$V_f^v(x) = \int_0^x G_{V_y}^{II}(x,\xi)q_v(\xi)\mathrm{d}\xi + \int_x^L G_{V_y}^I(x,\xi)q_v(\xi)\mathrm{d}\xi \tag{31b}$$

Being the functions $G_{My}(x,\xi)$ and $G_{Vy}(x,\xi)$ the bending moment and shear force Green's functions associated with the element presented in Fig. 6, i.e., the internal forces fields of the fixed axially non-uniform Timoshenko beam element subjected to a transverse point unit load located at ξ. Those functions also have two intervals and can be computed from $G_{yy}(x,\xi)$ and $G_{\theta y}(x,\xi)$ using Eqs. (1), or using simple statics based on the fact that their reactions are known (see Fig. 6):

$$G_{M_y}^I(x,\xi) = W_2^M(x)\psi_2^v(\xi) + W_3^M(x)\psi_3^v(\xi) \tag{32a}$$
$$G_{M_y}^{II}(x,\xi) = W_5^M(x)\psi_5^v(\xi) + W_6^M(x)\psi_6^v(\xi) \tag{32b}$$

and

$$G_{V_y}^I(x,\xi) = W_2^V(x)\psi_2^v(\xi) + W_3^V(x)\psi_3^v(\xi) \tag{33a}$$
$$G_{V_y}^{II}(x,\xi) = W_5^V(x)\psi_5^v(\xi) + W_6^V(x)\psi_6^v(\xi) \tag{33b}$$

where

$$W_2^M(x) = -x \tag{34a}$$
$$W_3^M(x) = 1 \tag{34b}$$
$$W_5^M(x) = -L + x \tag{34c}$$
$$W_6^M(x) = -1 \tag{34d}$$

and

$$W_2^V(x) = 1 \tag{35a}$$
$$W_3^V(x) = 0 \tag{35b}$$
$$W_5^V(x) = -1 \tag{35c}$$
$$W_6^V(x) = 0 \tag{35d}$$

By evaluating Eqs. (31) at the ends of the fixed element, the fixed-end forces (reactions) generated by the arbitrary external load $q_v(x)$ are obtained:

$$FY_i^{vf} = -V_f^v(0) = -\int_0^L \psi_2^v(x)q_v(x)\mathrm{d}x \tag{36a}$$
$$M_i^{vf} = -M_f^v(0) = -\int_0^L \psi_3^v(x)q_v(x)\mathrm{d}x \tag{36b}$$
$$FY_j^{vf} = V_f^v(L) = -\int_0^L \psi_5^v(x)q_v(x)\mathrm{d}x \tag{36c}$$
$$M_j^{vf} = M_f^v(L) = -\int_0^L \psi_6^v(x)q_v(x)\mathrm{d}x \tag{36d}$$

Being those equivalent to the ones used in the TFEM [19], and following the general form used in the FEM [57,60].

To understand the meaning of Eqs. (36), note that the reactions of the fixed beam presented in Fig. 6 are the negative of the shape

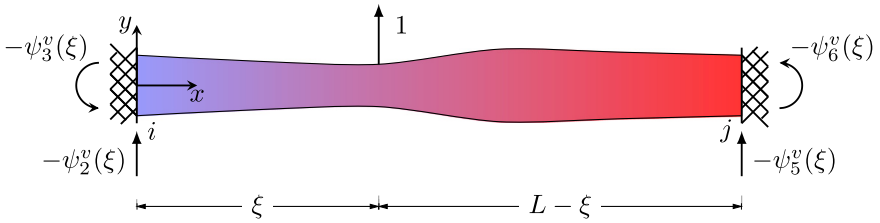

Fig. 6. Fixed axially non-uniform Timoshenko beam element subjected to a external unit point load, and its reactions.

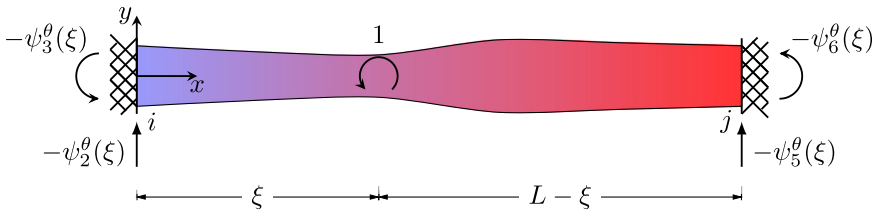

Fig. 7. Fixed axially non-uniform Timoshenko beam element subjected to a external unit bending moment, and its reactions.

functions $\psi_n^v(x)$ ($n = 2,3,5,6$), i.e., the reactions generated by the unit point load located at x (for ease of the discussion ξ has been changed to x). The term $-\psi_n^v(x)q_v(x)\mathrm{d}x$ can be interpreted as the reactions generated by the differential load $q_v(x)\mathrm{d}x$ located at x, and $-\int_0^L \psi_n^v(x)q_v(x)\mathrm{d}x$ is the superposition of the reactions generated by all the differential external loads from $x = 0$ to $x = L$.

3.3.2. Fixed response due to $q_\theta(x)$

To compute the response of the fixed axially non-uniform Timoshenko beam element subjected to the external bending moment $q_\theta(x)$ (see Fig. 5(b)), a similar approach to the one used in the previous section for the external load $q_v(x)$ will be followed. To do this, it is necessary to use the response of a fixed element subjected to a unit point bending moment as presented in Fig. 7.

This response includes the Green's functions $G_{y\theta}(x,\xi)$, $G_{\theta\theta}(x,\xi)$, $G_{M\theta}(x,\xi)$ and $G_{V\theta}(x,\xi)$, for the transverse displacement, rotation of the cross-section, bending moment, and shear force fields, respectively. Being those functions defined as:

$$G_{y\theta}^I(x,\xi) = W_2^v(x)\psi_2^\theta(\xi) + W_3^v(x)\psi_3^\theta(\xi) \tag{37a}$$
$$G_{y\theta}^{II}(x,\xi) = W_5^v(x)\psi_5^\theta(\xi) + W_6^v(x)\psi_6^\theta(\xi) \tag{37b}$$

$$G_{\theta\theta}^I(x,\xi) = W_2^\theta(x)\psi_2^\theta(\xi) + W_3^\theta(x)\psi_3^\theta(\xi) \tag{38a}$$
$$G_{\theta\theta}^{II}(x,\xi) = W_5^\theta(x)\psi_5^\theta(\xi) + W_6^\theta(x)\psi_6^\theta(\xi) \tag{38b}$$

$$G_{M\theta}^I(x,\xi) = W_2^M(x)\psi_2^\theta(\xi) + W_3^M(x)\psi_3^\theta(\xi) \tag{39a}$$
$$G_{M\theta}^{II}(x,\xi) = W_5^M(x)\psi_5^\theta(\xi) + W_6^M(x)\psi_6^\theta(\xi) \tag{39b}$$

and

$$G_{V\theta}^I(x,\xi) = W_2^V(x)\psi_2^\theta(\xi) + W_3^V(x)\psi_3^\theta(\xi) \tag{40a}$$
$$G_{V\theta}^{II}(x,\xi) = W_5^V(x)\psi_5^\theta(\xi) + W_6^V(x)\psi_6^\theta(\xi) \tag{40b}$$

From the comparison of the Green's functions of the fixed element subjected to the external transverse unit point load (Eqs. (26), (28), (32) and (33)) with those generated by the external unit point bending moment (Eqs. (37) to (40)), it is clear that the latter can be computed from the former by simply replacing the shape functions $\psi_n^v(\xi)$ by $\psi_n^\theta(\xi)$ ($n = 2,3,5,6$).

Following the same principle used in Section 3.3.1, the fixed transverse displacement, cross-section rotation, bending moment, and shear force fields caused by the external bending moment $q_\theta(x)$, are respectively:

$$v_f^\theta(x) = \int_0^x G_{y\theta}^{II}(x,\xi)q_\theta(\xi)\mathrm{d}\xi + \int_x^L G_{y\theta}^I(x,\xi)q_\theta(\xi)\mathrm{d}\xi \tag{41a}$$
$$\theta_f^\theta(x) = \int_0^x G_{\theta\theta}^{II}(x,\xi)q_\theta(\xi)\mathrm{d}\xi + \int_x^L G_{\theta\theta}^I(x,\xi)q_\theta(\xi)\mathrm{d}\xi \tag{41b}$$
$$M_f^\theta(x) = \int_0^x G_{M\theta}^{II}(x,\xi)q_\theta(\xi)\mathrm{d}\xi + \int_x^L G_{M\theta}^I(x,\xi)q_\theta(\xi)\mathrm{d}\xi \tag{41c}$$
$$V_f^\theta(x) = \int_0^x G_{V\theta}^{II}(x,\xi)q_\theta(\xi)\mathrm{d}\xi + \int_x^L G_{V\theta}^I(x,\xi)q_\theta(\xi)\mathrm{d}\xi \tag{41d}$$

From the internal forces fields presented in Eqs. (41c) and (41d), the fixed-end forces due to the external bending moment $q_\theta(x)$ are:

$$FY_i^{\theta f} = -V_f^\theta(0) = -\int_0^L \psi_2^\theta(x)q_\theta(x)\mathrm{d}x \tag{42a}$$
$$M_i^{\theta f} = -M_f^\theta(0) = -\int_0^L \psi_3^\theta(x)q_\theta(x)\mathrm{d}x \tag{42b}$$
$$FY_j^{\theta f} = V_f^\theta(L) = -\int_0^L \psi_5^\theta(x)q_\theta(x)\mathrm{d}x \tag{42c}$$
$$M_j^{\theta f} = M_f^\theta(L) = -\int_0^L \psi_6^\theta(x)q_\theta(x)\mathrm{d}x \tag{42d}$$

4. Formulation of the GFSM for the axially non-uniform rod element

A summary of the GFSM formulation for the axially non-uniform rod element is presented in this section. A more detailed explanation is presented in [46].

For this element, the axial force field is calculated from the axial displacement field as:

$$P(x) = AE(x)\frac{\mathrm{d}u}{\mathrm{d}x}(x) \tag{43}$$

where $AE(x) = A(x)E(x)$ is the axial rigidity.

The axial displacement and axial force fields are decomposed into their homogeneous and fixed parts, as follows:

$$u(x) = u_h(x) + u_f(x) \tag{44a}$$
$$P(x) = P_h(x) + P_f(x) \tag{44b}$$

being $u_h(x)$ and $u_f(x)$ the homogeneous and fixed axial displacement fields, and $P_h(x)$ and $P_f(x)$ the homogeneous and fixed axial force fields, respectively.

Homogeneous response

The homogeneous axial displacement and axial force fields are computed as:

$$u_h(x) = \psi_1^u(x)u_i + \psi_4^u(x)u_j \tag{45a}$$

$$P_h(x) = \psi_1^P(x)u_i + \psi_4^P(x)u_j \tag{45b}$$

Where $\psi_1^u(x)$ and $\psi_4^u(x)$ are the axial displacement shape functions, whereas $\psi_1^P(x)$ and $\psi_4^P(x)$ are the axial force shape functions, defined respectively as:

$$\psi_1^u(x) = 1 - \frac{\int_0^x \frac{1}{AE(\kappa)}\mathrm{d}\kappa}{\int_0^L \frac{1}{AE(x)}\mathrm{d}x} \tag{46a}$$

$$\psi_4^u(x) = \frac{\int_0^x \frac{1}{AE(\kappa)}\mathrm{d}\kappa}{\int_0^L \frac{1}{AE(x)}\mathrm{d}x} \tag{46b}$$

and

$$\psi_1^P(x) = -\frac{1}{\int_0^L \frac{1}{AE(x)}\mathrm{d}x} \tag{47a}$$

$$\psi_4^P(x) = \frac{1}{\int_0^L \frac{1}{AE(x)}\mathrm{d}x} \tag{47b}$$

Evaluating Eq. (45b) at $x = 0$ and $x = L$ yields the exact relation between the homogeneous forces and displacements at the element ends:

$$\begin{Bmatrix} FX_i^h \\ FX_j^h \end{Bmatrix} = \begin{Bmatrix} -P_h(0) \\ P_h(L) \end{Bmatrix} = \begin{bmatrix} k_{11} & k_{14} \\ k_{41} & k_{44} \end{bmatrix} \begin{Bmatrix} u_i \\ u_j \end{Bmatrix} \tag{48}$$

where:

$$k_{11} = k_{44} = -k_{14} = -k_{41} = \frac{1}{\int_0^L \frac{1}{AE(x)}\mathrm{d}x} \tag{49}$$

Being the analytic stiffness matrix of the axially non-uniform rod element, the 2×2 matrix presented in Eq. (48).

Fixed response

The fixed axial displacement and the fixed axial force fields are computed as follows:

$$u_f(x) = \int_0^x G_{xx}^{II}(x,\xi)p(\xi)\mathrm{d}\xi + \int_x^L G_{xx}^{I}(x,\xi)p(\xi)\mathrm{d}\xi \tag{50a}$$

$$P_f(x) = \int_0^x G_{Px}^{II}(x,\xi)p(\xi)\mathrm{d}\xi + \int_x^L G_{Px}^{I}(x,\xi)p(\xi)\mathrm{d}\xi \tag{50b}$$

Where $G_{xx}(x,\xi)$ and $G_{Px}(x,\xi)$ are the axial displacement and the axial force Green's functions, respectively, defined as (see Fig. 8):

$$G_{xx}(x,\xi) = \begin{cases} G_{xx}^{I}(x,\xi) = W_1^u(x)\psi_1^u(\xi) & 0 < x \le \xi \\ G_{xx}^{II}(x,\xi) = W_4^u(x)\psi_4^u(\xi) & \xi \le x < L \end{cases} \tag{51}$$

being

$$W_1^u(x) = \left[\int_0^L \frac{1}{AE(x)}\mathrm{d}x\right]\psi_4^u(x) \tag{52a}$$

$$W_4^u(x) = \left[\int_0^L \frac{1}{AE(x)}\mathrm{d}x\right]\psi_1^u(x) \tag{52b}$$

and

$$G_{Px}(x,\xi) = \begin{cases} G_{Px}^{I}(x,\xi) = W_1^P(x)\psi_1^u(\xi) & 0 < x < \xi \\ G_{Px}^{II}(x,\xi) = W_4^P(x)\psi_4^u(\xi) & \xi < x < L \end{cases} \tag{53}$$

where

$$W_1^P(x) = 1 \tag{54a}$$

$$W_4^P(x) = -1 \tag{54b}$$

The fixed-end forces are computed from Eq. (50b) as:

$$\begin{Bmatrix} FX_i^f \\ FX_j^f \end{Bmatrix} = \begin{Bmatrix} -P_f(0) \\ P_f(L) \end{Bmatrix} = -\begin{Bmatrix} \int_0^L \psi_1(x)p(x)\mathrm{d}x \\ \int_0^L \psi_4(x)p(x)\mathrm{d}x \end{Bmatrix} \tag{55}$$

5. Formulation of the GFSM for the axially non-uniform Timoshenko frame element

The formulation of the GFSM for the axially non-uniform Timoshenko frame element presented in Fig. 1 is obtained by superposing the formulations of the axially non-uniform Timoshenko beam element (Section 3) and the axially non-uniform rod element (Section 4). The exact relation between forces and displacements at the frame element ends is:

$$\begin{Bmatrix} FX_i \\ FY_i \\ M_i \\ FX_j \\ FY_j \\ M_j \end{Bmatrix} = \begin{bmatrix} k_{11} & 0 & 0 & k_{14} & 0 & 0 \\ 0 & k_{22} & k_{23} & 0 & k_{25} & k_{26} \\ 0 & k_{32} & k_{33} & 0 & k_{35} & k_{36} \\ k_{41} & 0 & 0 & k_{44} & 0 & 0 \\ 0 & k_{52} & k_{53} & 0 & k_{55} & k_{56} \\ 0 & k_{62} & k_{63} & 0 & k_{65} & k_{66} \end{bmatrix} \begin{Bmatrix} u_i \\ v_i \\ \theta_i \\ u_j \\ v_j \\ \theta_j \end{Bmatrix} - \begin{Bmatrix} \int_0^L \psi_1^u(x)p(x)\mathrm{d}x \\ \int_0^L \left[\psi_2^v(x)q_v(x) + \psi_2^\theta(x)q_\theta(x)\right]\mathrm{d}x \\ \int_0^L \left[\psi_3^v(x)q_v(x) + \psi_3^\theta(x)q_\theta(x)\right]\mathrm{d}x \\ \int_0^L \psi_4^u(x)p(x)\mathrm{d}x \\ \int_0^L \left[\psi_5^v(x)q_v(x) + \psi_5^\theta(x)q_\theta(x)\right]\mathrm{d}x \\ \int_0^L \left[\psi_6^v(x)q_v(x) + \psi_6^\theta(x)q_\theta(x)\right]\mathrm{d}x \end{Bmatrix} \tag{56}$$

The axial displacement, transverse displacement, and cross-section rotation fields are obtained from Eqs. (57) to (59), respectively, while the axial force, bending moment, and shear force fields are computed from Eqs. (60) to (62), respectively. It is evident that in the case of a FEM formulation employing analytic shape functions and stiffness matrices, such as TFEM, the GFSM can be utilized to "fix" their results as an additional post-processing step during the analysis, involving the addition of the fixed response for each element.

$$u(x) = \psi_1^u(x)u_i + \psi_4^u(x)u_j + \int_0^x G_{xx}^{II}(x,\xi)p(\xi)\mathrm{d}\xi + \int_x^L G_{xx}^{I}(x,\xi)p(\xi)\mathrm{d}\xi \tag{57}$$

$$\begin{aligned} v(x) = {} & \psi_2^v(x)v_i + \psi_3^v(x)\theta_i + \psi_5^v(x)v_j + \psi_6^v(x)\theta_j \\ & + \int_0^x \left[G_{yy}^{II}(x,\xi)q_v(\xi) + G_{y\theta}^{II}(x,\xi)q_\theta(\xi)\right]\mathrm{d}\xi \\ & + \int_x^L \left[G_{yy}^{I}(x,\xi)q_v(\xi) + G_{y\theta}^{I}(x,\xi)q_\theta(\xi)\right]\mathrm{d}\xi \end{aligned} \tag{58}$$

$$\begin{aligned} \theta(x) = {} & \psi_2^\theta(x)v_i + \psi_3^\theta(x)\theta_i + \psi_5^\theta(x)v_j + \psi_6^\theta(x)\theta_j \\ & + \int_0^x \left[G_{\theta y}^{II}(x,\xi)q_v(\xi) + G_{\theta\theta}^{II}(x,\xi)q_\theta(\xi)\right]\mathrm{d}\xi \\ & + \int_x^L \left[G_{\theta y}^{I}(x,\xi)q_v(\xi) + G_{\theta\theta}^{I}(x,\xi)q_\theta(\xi)\right]\mathrm{d}\xi \end{aligned} \tag{59}$$

$$P(x) = \psi_1^P(x)u_i + \psi_4^P(x)u_j + \int_0^x G_{Px}^{II}(x,\xi)p(\xi)\mathrm{d}\xi + \int_x^L G_{Px}^{I}(x,\xi)p(\xi)\mathrm{d}\xi \tag{60}$$

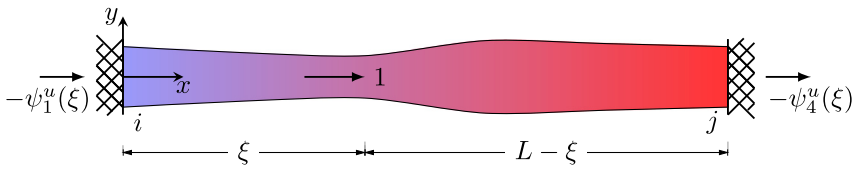

Fig. 8. Fixed axially non-uniform rod element subjected to an external axial unit point load, and its reactions.

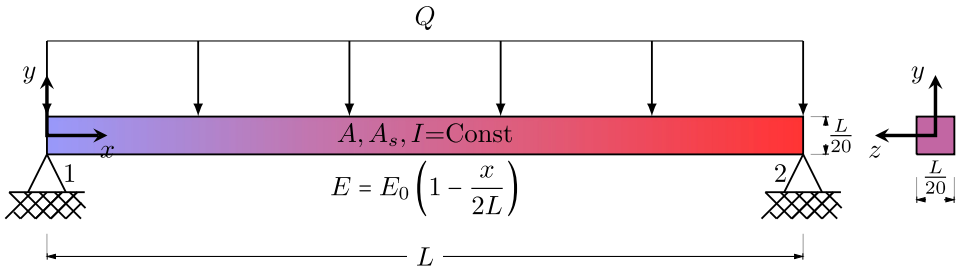

Fig. 9. Simple supported axially non-uniform Timoshenko beam.

$$M(x) = \psi_2^M(x)v_i + \psi_3^M(x)\theta_i + \psi_5^M(x)v_j + \psi_6^M(x)\theta_j + \int_0^x \left[G^{II}_{M_y}(x,\xi)q_v(\xi) + G^{II}_{M\theta}(x,\xi)q_\theta(\xi)\right]\mathrm{d}\xi + \int_x^L \left[G^{I}_{M_y}(x,\xi)q_v(\xi) + G^{I}_{M\theta}(x,\xi)q_\theta(\xi)\right]\mathrm{d}\xi \tag{61}$$

$$V(x) = \psi_2^V(x)v_i + \psi_3^V(x)\theta_i + \psi_5^V(x)v_j + \psi_6^V(x)\theta_j + \int_0^x \left[G^{II}_{V_y}(x,\xi)q_v(\xi) + G^{II}_{V\theta}(x,\xi)q_\theta(\xi)\right]\mathrm{d}\xi + \int_x^L \left[G^{I}_{V_y}(x,\xi)q_v(\xi) + G^{I}_{V\theta}(x,\xi)q_\theta(\xi)\right]\mathrm{d}\xi \tag{62}$$

For interested readers, a step-by-step procedure for implementing the GFSM is presented in [46], which has been omitted in this paper due to its close relation with the FEM.

6. Examples

6.1. Example 1

Compute the response of the axially non-uniform Timoshenko beam presented in Fig. 9, which has square cross-section with sides of $L/20$, linear elastic material with Poisson's ratio of 0.2, and linearly varying Young's modulus define as $E(x) = E_0\left(1-\frac{x}{2L}\right)$.

Solution

The main mechanical and geometric properties of the beam are:

$$G(x) = \frac{E(x)}{2(1+\nu)} = \frac{5}{12}E_0\left(1-\frac{x}{2L}\right) \tag{63a}$$

$$\kappa = \frac{5+5\nu}{6+5\nu} = \frac{6}{7} \tag{63b}$$

$$A = \frac{L^2}{400} \tag{63c}$$

$$I = \frac{L^4}{1920000} \tag{63d}$$

Where the value of κ has been computed following [61,62].

The transverse displacement and cross-section rotation fields obtained using the GFSM are presented in Eqs. (64) and (65), respectively, with the former being the same as presented in Eq. (42) of [35].

$$v(x) = \frac{Q}{E_0}\left\{\ln\left(1-\frac{x}{2L}\right)\left(-7683360 + 3840000\frac{x}{L}\right) - [3843360\ln(2) + 1280000]\frac{x}{L} + 960000\left(\frac{x}{L}\right)^2 + 320000\left(\frac{x}{L}\right)^3\right\} \tag{64}$$

$$\theta(x) = \frac{Q}{E_0 L}\left\{3840000\ln\left(1-\frac{x}{2L}\right) + 1920000\frac{x}{L} + 960000\left(\frac{x}{L}\right)^2 - 3843360\ln(2) + 2562240\right\} \tag{65}$$

By substituting the transverse displacement and cross-section rotation fields presented in Eqs. (64) and (65), respectively, into Eqs. (1), there are obtained the internal forces fields:

$$M(x) = \frac{QL^2}{2}\left[\frac{x}{L} - \left(\frac{x}{L}\right)^2\right] \tag{66a}$$

$$V(x) = QL\left(-\frac{1}{2} + \frac{x}{L}\right) \tag{66b}$$

From the internal forces fields and employing the fundamental kinematic equations for Timoshenko beams, the fields of normal (σ_{xx}) and shear stresses (τ_{xy}) can be computed as follows:

$$\sigma_{xx}(x,y) = -\frac{M(x)y}{I} = -960000\left[\frac{x}{L} - \left(\frac{x}{L}\right)^2\right]\frac{y}{L}\frac{Q}{L} \tag{67a}$$

$$\tau_{xy}(x) = \frac{V(x)}{A_s} = \frac{700}{3}\left(-1+2\frac{x}{L}\right)\frac{Q}{L} \tag{67b}$$

In Fig. 10, the schematic representations of these stress fields are presented.

Source file

From the following links can be downloaded the Python source file used to solve this example: https://figshare.com/s/5a9f781626f433a9057e, DOI http://dx.doi.org/10.6084/m9.figshare.24324505.

6.2. Example 2

Compute the response of the non-uniform Timoshenko beam presented in Fig. 11. The beam features a variable circular cross-section with linearly varying radius from $L/40$ at $x = 0$ to $3L/80$ at $x = L$, and has a homogeneous linear elastic material with a Poisson's ratio of 0.2, and Young's modulus E.

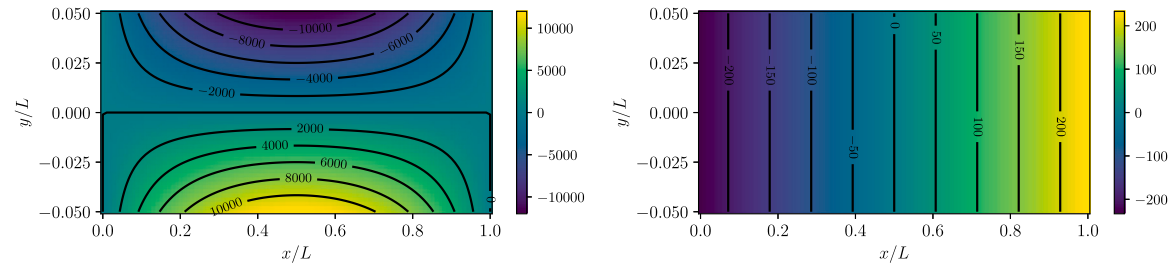

(a) $\frac{\sigma_{xx}(x,y)}{Q/L}$. (b) $\frac{\tau_{xy}(x)}{Q/L}$.

Fig. 10. Dimensionless normal and shear stress fields.

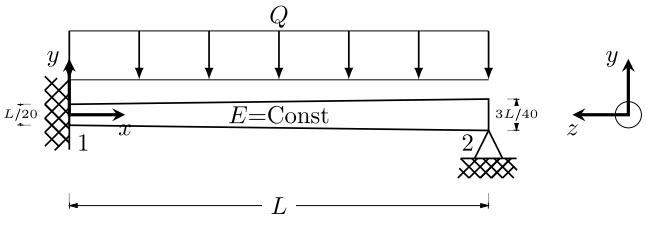

Fig. 11. Non-uniform Timoshenko beam.

Solution

The geometric and mechanical properties required for solving this example are summarized in the following equations:

$$r(x) = \frac{L}{40}\left(1 + \frac{x}{2L}\right) \tag{68a}$$

$$A(x) = \frac{\pi L^2}{1600}\left(1 + \frac{x}{2L}\right)^2 \tag{68b}$$

$$I(x) = \frac{\pi L^4\left(1 + \frac{x}{2L}\right)^4}{10240000} \tag{68c}$$

$$G = \frac{E}{2(1+\nu)} = \frac{5}{12}E \tag{68d}$$

$$\kappa = \frac{6 + 12\nu + 6\nu^2}{7 + 12\nu + 4\nu^2} = \frac{216}{239} \tag{68e}$$

Where the value of κ has been computed following [61,62].

External load

The external load applied to the beam is defined as:

$$q_v(x) = -Q \qquad 0 < x < L \tag{69}$$

To shorten the solution, all results will be presented in decimal format. For exact values, refer to the Python source file.

Calculation of the generalized nodal displacements

From the fact that $M_2 = 0$, using the formulation of the GFSM it is obtained:

$$0 = 4.11447 \times 10^{-6} EL^3\theta_2 - 0.11309QL^2 \quad \therefore \quad \theta_2 = 27485.92250\frac{Q}{EL} \tag{70}$$

Calculation of the displacement fields

Using Eqs. (58) and (59), the transverse displacement and cross-section rotation fields are computed:

$$v(x) = \frac{Q}{E}\left[\frac{26712312.6584 + 16930321.2296\frac{x}{L}}{\left(1 + \frac{x}{2L}\right)^2} + 26081355.7295\ln\left(1 + \frac{x}{2L}\right) - 26712312.6584 - 3259493.2345\frac{x}{L}\right] \tag{71}$$

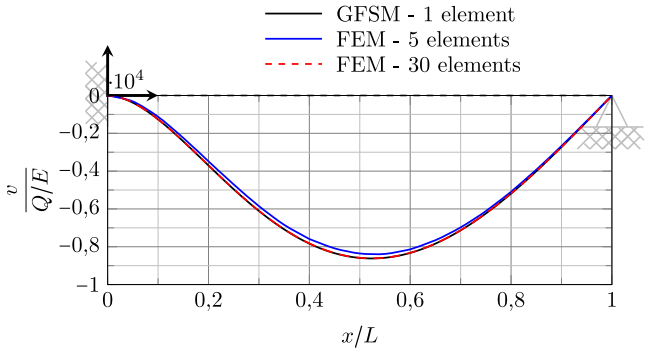

Fig. 12. Transverse displacement field using the GFSM with 1 element, and the FEM with 5 and 30 uniform elements.

$$\theta(x) = \frac{Q}{EL}\frac{\frac{x}{L}\left[-407436.6543\left(\frac{x}{L}\right)^2 + 814873.3086\frac{x}{L} - 314671.6659\right]}{0.125\left(\frac{x}{L}\right)^3 + 0.75\left(\frac{x}{L}\right)^2 + 1.5\frac{x}{L} + 1} \tag{72}$$

Fig. 12 compares the displacement field obtained using the GFSM with a single element, and two FEM discretizations consisting of uniform elements using 5 and 30 elements employing the OpenSees software [63], demonstrating excellent agreement between the GFSM and the denser FEM mesh solutions.

Calculation of the internal forces fields

From the displacement and cross-section rotation fields, the internal forces fields are computed using Eqs. (1):

$$V(x) = \left(-0.59654 + \frac{x}{L}\right)QL \tag{73a}$$

$$M(x) = \left[-0.09654 + 0.59654\frac{x}{L} - 0.5\left(\frac{x}{L}\right)^2\right]QL^2 \tag{73b}$$

The reactions are computed based on the internal forces fields as follows:

$$FY_1 = -V(0) = 0.59654QL \tag{74a}$$

$$M_1 = -M(0) = 0.09654QL^2 \tag{74b}$$

$$FY_2 = V(L) = 0.40346QL \tag{74c}$$

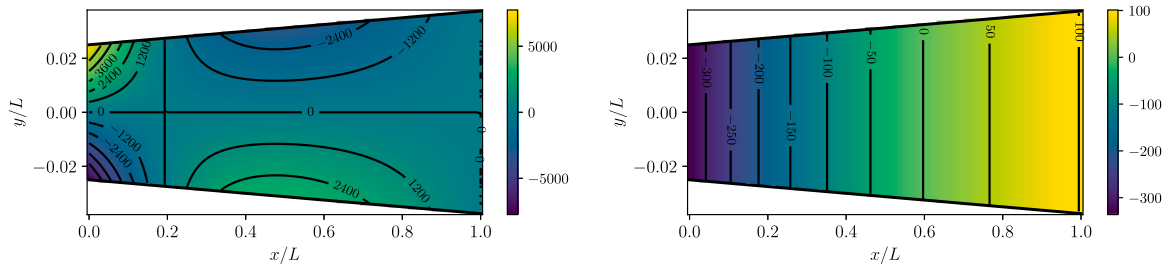

(a) $\frac{\sigma_{xx}(x,y)}{Q/L}$. (b) $\frac{\tau_{xy}(x)}{Q/L}$.

Fig. 13. Dimensionless normal and shear stress fields.

Calculation of the stress fields

The normal and shear stress fields are computed from the internal forces fields as follows:

$$\sigma_{xx}(x,y) = -\frac{M(x)y}{I} = \frac{\left[314671.6659 - 1944418.2832\frac{x}{L} + 1629746.6173\left(\frac{x}{L}\right)^2\right]\frac{y}{L}}{1 + 2\frac{x}{L} + 1.5\left(\frac{x}{L}\right)^2 + 0.5\left(\frac{x}{L}\right)^3 + 0.0625\left(\frac{x}{L}\right)^4}\frac{Q}{L} \tag{75}$$

$$\tau_{xy}(x,y) = \frac{V(x)}{A_s(x)} = \frac{-336.1661 + 563.5264\frac{x}{L}}{1 + \frac{x}{L} + 0.25\left(\frac{x}{L}\right)^2}\frac{Q}{L} \tag{76}$$

While their schematic representations are presented in Figs. 13.

Source file

From the following links can be downloaded the Python source file used to solve this example: https://figshare.com/s/131a7c434112d891a241, DOI http://dx.doi.org/10.6084/m9.figshare.25175345.

6.3. Example 3

Compute the response of the axially non-uniform Timoshenko frame presented in Fig. 14(a), which has 3 solid uniform elements with circular cross-section of radius equal to 0.3 m, linear elastic material with Poisson's ratio of 0.2, and axially varying Young's modulus defined for each element as $E_E(x'_E) = E^0_E \exp(\alpha_E x'_E)$ (see Table 1 for the vales of E^0_E and α_E), being x'_E the axial local axis of the element E (see Fig. 14(b)).

Table 1
Properties to define the Young's modulus of each element.

Element	$E^0_E = E_E(0)$	α_E
A	2×10^7	ln(3/2)/5
B	3×10^7	ln(2/3)/4
C	2×10^7	ln(3/2)/5

Calculation of the generalized nodal displacements

$$\begin{Bmatrix}0\\0\\0\\0\\0\\0\end{Bmatrix} = \begin{bmatrix} 2797425 & 653353 & 31080 & -2292851 & 0 & 0 \\ 653353 & 949892 & 79473 & 0 & -64196 & 89804 \\ 31080 & 79473 & 350779 & 0 & -102783 & 92195 \\ -2292851 & 0 & 0 & 2797425 & -653353 & 27156 \\ 0 & -64196 & -102783 & -653353 & 949892 & -69437 \\ 0 & 89804 & 92195 & 27156 & -69437 & 287313 \end{bmatrix}\begin{Bmatrix}u_2\\v_2\\\theta_2\\u_3\\v_3\\\theta_3\end{Bmatrix} + \begin{Bmatrix}-0.962\\102.336\\12.575\\6.188\\43.202\\-5.455\end{Bmatrix} \tag{77}$$

Being its solution:

$$\begin{Bmatrix}u_2\\v_2\\\theta_2\\u_3\\v_3\\\theta_3\end{Bmatrix} = \begin{Bmatrix}2.64598\times10^{-4}\ \text{m}\\-2.93752\times10^{-4}\ \text{m}\\9.70044\times10^{-6}\ \text{rad}\\2.38833\times10^{-4}\ \text{m}\\1.08122\times10^{-4}\ \text{m}\\1.11248\times10^{-4}\ \text{rad}\end{Bmatrix} \tag{78}$$

Computation of the reactions

$$\begin{Bmatrix}FX_1\\FY_1\\M_1\\FX_4\\FY_4\\M_4\end{Bmatrix} = \begin{bmatrix} -504574 & -653353 & -31080 & 0 & 0 & 0 \\ -653353 & -885696 & 23310 & 0 & 0 & 0 \\ 27156 & -20367 & 59627 & 0 & 0 & 0 \\ 0 & 0 & 0 & -504574 & 653353 & -27156 \\ 0 & 0 & 0 & 653353 & -885696 & -20367 \\ 0 & 0 & 0 & 31080 & 23310 & 59627 \end{bmatrix}\begin{Bmatrix}u_2\\v_2\\\theta_2\\u_3\\v_3\\\theta_3\end{Bmatrix} + \begin{Bmatrix}0.962\\8.932\\5.941\\-6.188\\10.530\\-3.479\end{Bmatrix} = \begin{Bmatrix}59.075\ \text{kN}\\96.458\ \text{kN}\\19.687\ \text{kN m}\\-59.075\ \text{kN}\\68.542\ \text{kN}\\13.098\ \text{kN m}\end{Bmatrix} \tag{79}$$

Calculation of the displacement fields

Fig. 15 compares the deformed shapes of the structure obtained using the GFSM with 3 elements, and the FEM with 45 and 360 elements using the OpenSees software [63], a scale factor of 3000 has been used. It is clear that the two methods have an excellent agreement, especially for the denser FEM mesh.

Calculation of the internal forces fields

Figs. 16 compares the internal forces fields computed with the GFSM and the two previously mentioned FEM meshes.

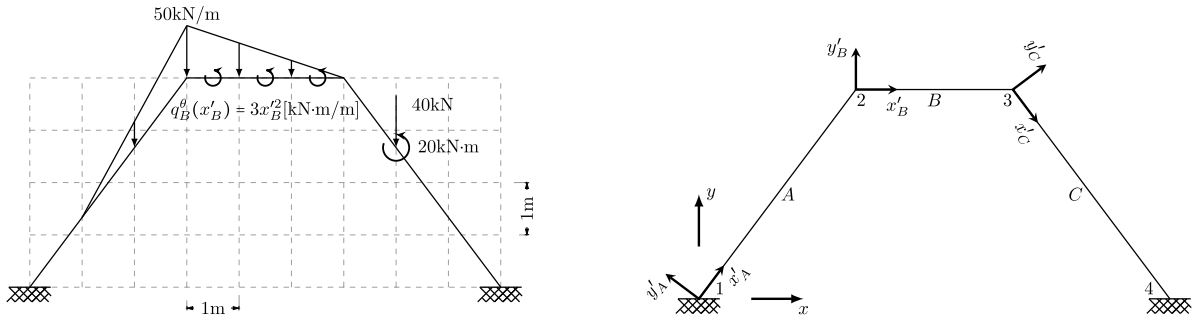

(a) Model. (b) Discretization.

Fig. 14. Model and discretization of the axially non-uniform Timoshenko frame.

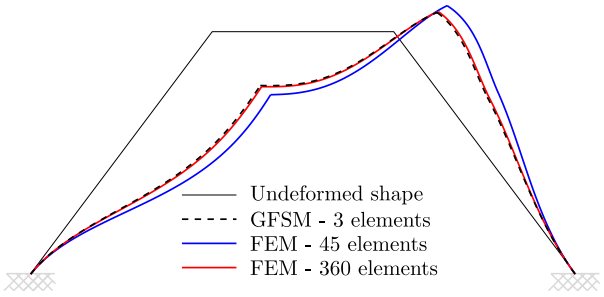

Fig. 15. Deformed shape of the structure with a scale factor of 3000, using the GFSM with 3 elements presented in Fig. 14(b), and two FEM discretizations using 45 and 360 FEs (15 and 120 FEs per structural member, respectively).

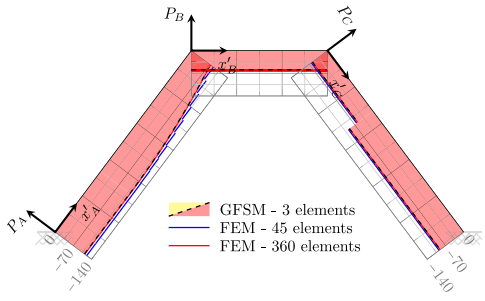

(a) Axial force [kN].

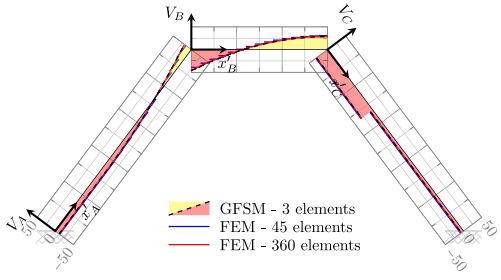

(b) Shear force [kN].

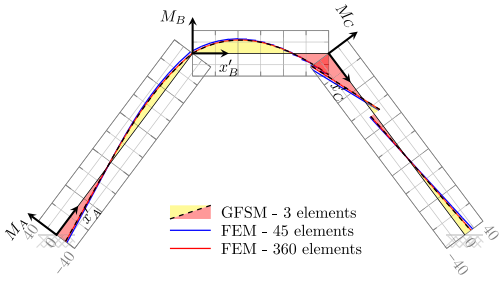

(c) Bending moment [kN·m].

Fig. 16. Internal forces fields computed using the GFSM with 3 elements (dashed black line) and the FEM using 45 and 360 FEs (15 and 45 FEs by structural element, respectively).

Again, the agreement between GFSM and the denser FEM mesh is excellent.

Calculation of the stress fields

From the internal force fields, the normal and shear stresses can be easily calculated as indicated in Eqs. (67). For this example, their figures are not presented due to the high saturation of the colormap and contour lines. However, it is clear that the normal stress exhibits a linear variation with the local y'_E axis of each element, following the same axial variation as the bending moment field $M_E\left(x_E\right)$. Meanwhile, the shear stress remains constant across the entire cross-section and shares the same axial variation as the shear force field $V_E\left(x_E\right)$.

Source file

From the following links can be downloaded the Python source file used to solve this example: https://figshare.com/s/c46641feafbcdcacd749, DOI http://dx.doi.org/10.6084/m9.figshare.25176044.

7. Conclusions

1. This paper presents the formulation of the GFSM for the static analysis of arbitrary axially non-uniform Timoshenko beams and frames subjected to general external loads and bending moments, enabling the calculation of their closed-form solutions.
2. The GFSM is an analytic mesh-reduction method that is closely related to the FEM and shares with it fundamental features such as stiffness matrices, shape functions, and fixed-end forces. In the case of a FEM formulation that uses analytic shape functions and stiffness matrices, such as the TFEM, the GFSM can be used to "fix" the FEM results just as an additional post-processing step.
3. Because the formulation of the GFSM is based on the exact solutions of the governing differential equations (strong formulation), instead of an approximated weak formulation like in the FEM, it always obtains 100% consistent solutions. This eliminates common problems such as shear locking [64], sawtooth behavior in the internal forces fields, or discrepancies between the internal forces fields and the elements end forces, common in FEM solutions.
4. To demonstrate the benefits of the GFSM for obtaining closed-form solutions of axially non-uniform Timoshenko beams and frames, three examples were presented. The first example computed the response of a single-span, axially non-uniform Timoshenko beam and compared it with the analytical solution presented in [35]. The second example showed the solution of a beam with a variable cross-section and compared it to the FEM solution, while the third example calculated the response of a axially non-uniform Timoshenko plane frame and compared it to the FEM solution using very dense meshes.

CRediT authorship contribution statement

Juan Camilo Molina-Villegas: Conceptualization, Methodology, Validation, Writing – original draft. **Jorge Eliecer Ballesteros Ortega:** Conceptualization, Methodology, Writing – review & editing. **Simón Benítez Soto:** Software, Validation, Writing – review & editing.

Declaration of competing interest

The authors declare that they have no known competing financial interests or personal relationships that could have appeared to influence the work reported in this paper.

Nomenclature

Geometric parameters

$\kappa(x)$	Shear coefficient
$A(x)$	Cross-sectional area
$A_s(x)$	Cross-sectional shear area
$I(x)$	Moment of inertia of the cross-section about the z-axis.
L	Element length
x, y, z	Element local axes in axial x, and transverse y, z directions

Mechanical parameters

$\mathcal{I}_n(x)$	Integrals of the axial, flexural, and shear rigidity of the element presented in Eqs. (11) ($n = 1, \ldots, 5$)
$\nu(x)$	Poisson's ratio
$E(x)$	Young's modulus
$G(x)$	Shear modulus

Displacement field parameters

$\psi_n^u(x)$	Axial displacement field shape functions ($n = 1, 4$)
$\psi_n^v(x)$	Transverse displacement field shape functions ($n = 2, 3, 5, 6$)
$\psi_n^\theta(x)$	Cross-section rotation field shape functions ($n = 2, 3, 5, 6$)
$\theta(x)$	Cross-section rotation field
$\theta_f(x)$	Fixed cross-section rotation field
$\theta_f^v(x)$	Fixed cross-section rotation field generated by $q_v(x)$
$\theta_f^\theta(x)$	Fixed cross-section rotation field generated by $q_\theta(x)$
$\theta_h(x)$	Homogeneous cross-section rotation field
θ_n	Cross-section rotation at the end of the element connected with the joint n. In the general case, $n = i$ for the start of the element, and $n = j$ for the end of the element
$u(x)$	Axial displacement field
$u_f(x)$	Fixed axial displacement field
$u_h(x)$	Homogeneous axial displacement field
u_n	Axial displacement at the end of the element connected with the joint n. In the general case, $n = i$ for the start of the element, and $n = j$ for the end of the element
$v(x)$	Transverse displacement field
$v_f(x)$	Fixed transverse displacement field
$v_f^v(x)$	Fixed transverse displacement field generated by $q_v(x)$
$v_f^\theta(x)$	Fixed transverse displacement field generated by $q_\theta(x)$
$v_h(x)$	Homogeneous transverse displacement field
v_n	Transverse displacement at the end of the element connected with the joint n. In the general case, $n = i$ for the start of the element, and $n = j$ for the end of the element

External loads and internal forces parameters

$\sigma(x, y)$	Normal stress field
$\tau(x)$	Shear stress field
FY_n	Element end force in the y-axis direction, $n = i$ for the start and $n = j$ for the end of the element
FY_n^f	Fixed element end force in the y-axis direction, $n = i$ for the start and $n = j$ for the end of the element
FY_n^h	Homogeneous element end force in the y-axis direction, $n = i$ for the start and $n = j$ for the end of the element
$FY_n^{\theta f}$	Fixed element end force in the y-axis direction caused by $q_\theta(x)$, $n = i$ for the start and $n = j$ for the end of the element

FY_n^{vf} Fixed element end force in the y-axis direction caused by $q_v(x)$, $n = i$ for the start and $n = j$ for the end of the element
$M(x)$ Bending moment field
$M_f(x)$ Fixed bending moment field
$M_f^v(x)$ Fixed bending moment field caused by $q_v(x)$
$M_f^\theta(x)$ Fixed bending moment field caused by $q_\theta(x)$
$M_h(x)$ Homogeneous bending moment field
M_n Element end bending moment, $n = i$ for the start and $n = j$ for the end of the element
M_n^f Fixed element end bending moment, $n = i$ for the start and $n = j$ for the end of the element
M_n^h Homogeneous element end bending moment, $n = i$ for the start and $n = j$ for the end of the element
$M_n^{\theta f}$ Fixed element end bending moment caused by $q_\theta(x)$, $n = i$ for the start and $n = j$ for the end of the element
M_n^{vf} Fixed element end bending caused by $q_v(x)$, $n = i$ for the start and $n = j$ for the end of the element
$P(x)$ Axial force field
$p(x)$ Axially external load field (positive in x-axis direction)
$P_f(x)$ Fixed axial force field
$P_h(x)$ Homogeneous axial force field
$q_v(x)$ Transverse external load field (positive in y-axis direction)
$q_\theta(x)$ External bending moment field (positive in z-axis direction)
$V(x)$ Shear force field
$V_f(x)$ Fixed shear force field
$V_f^v(x)$ Fixed shear force field caused by $q_v(x)$
$V_f^\theta(x)$ Fixed shear force field caused by $q_\theta(x)$
$V_h(x)$ Homogeneous shear force field

Green's functions

$G_{R\theta}(x,\xi)$ Green's function for the transverse displacement ($R = y$), cross-section rotation ($R = \theta$), bending moment ($R = M$), and shear force ($R = V$) fields of a fixed beam subjected to an external unit point bending moment (see Fig. 7).
$G_{Rx}(x,\xi)$ Green's function for the axial displacement ($R = x$) and the axial force ($R = P$) fields of a fixed beam subjected to an external unit point longitudinal load (see Fig. 8).
$G_{Ry}(x,\xi)$ Green's function for the transverse displacement ($R = y$), cross-section rotation ($R = \theta$), bending moment ($R = M$), and shear force ($R = V$) fields of a fixed beam subjected to an external unit point transverse load (see Fig. 6).
$W_n^M(x)$ Functions used to compute the Green's functions $G_{My}(x,\xi)$ and $G_{M\theta}(x,\xi)$ ($n = 2,3,5,6$)
$W_n^P(x)$ Functions used to compute the Green's function $G_{Px}(x,\xi)$ ($n = 1,4$)
$W_n^u(x)$ Functions used to compute the Green's function $G_{xx}(x,\xi)$ ($n = 1,4$)
$W_n^V(x)$ Functions used to compute the Green's functions $G_{Vy}(x,\xi)$ and $G_{V\theta}(x,\xi)$ ($n = 2,3,5,6$)
$W_n^v(x)$ Functions used to compute the Green's functions $G_{yy}(x,\xi)$ and $G_{y\theta}(x,\xi)$ ($n = 2,3,5,6$)
$W_n^\theta(x)$ Functions used to compute the Green's functions $G_{\theta y}(x,\xi)$ and $G_{\theta\theta}(x,\xi)$ ($n = 2,3,5,6$)

Data availability

No data was used for the research described in the article. The Python code used for the elaboration of both examples is presented at the end of each one.

References

[1] El-Mezaini N, Balkaya C, Çitipitioğlu E. Analysis of frames with nonprismatic members. J Struct Eng 1991;117(6):1573–92. http://dx.doi.org/10.1061/(ASCE)0733-9445(1991)117:6(1573).
[2] Mercuri V, Balduzzi G, Asprone D, Auricchio F. Structural analysis of non-prismatic beams: Critical issues, accurate stress recovery, and analytical definition of the finite element (fe) stiffness matrix. Eng Struct 2020;213:110252. http://dx.doi.org/10.1016/j.engstruct.2020.110252, https://www.sciencedirect.com/science/article/pii/S0141029619321601.
[3] Birman V, Byrd LW. Modeling and analysis of functionally graded materials and structures. Appl Mech Rev 2007;60(5):195–216. http://dx.doi.org/10.1115/1.2777164.
[4] Saleh B, Jiang J, Fathi R, Al-hababi T, Xu Q, Wang L, et al. 30 Years of functionally graded materials: An overview of manufacturing methods, applications and future challenges. Composites B 2020;201:108376. http://dx.doi.org/10.1016/j.compositesb.2020.108376, https://www.sciencedirect.com/science/article/pii/S1359836820334247.
[5] Jayachandiran G, Ramamoorthy M. Advancements in manufacturing and vibration analysis of functionally graded polymer composites: A review. Mech Adv Mater Struct 2023;1–20. http://dx.doi.org/10.1080/15376494.2023.2289086.
[6] Gupta A, Talha M. Recent development in modeling and analysis of functionally graded materials and structures. Prog Aerosp Sci 2015;79:1–14. http://dx.doi.org/10.1016/j.paerosci.2015.07.001, https://www.sciencedirect.com/science/article/pii/S0376042115000561.
[7] Akshaya S, Prakash A, Bharati Raj J. Applications of functionally graded materials in structural engineering—a review. In: National conference on structural engineering and construction management. Springer; 2020, p. 553–66.
[8] Cao D, Gao Y, Yao M, Zhang W. Free vibration of axially functionally graded beams using the asymptotic development method. Eng Struct 2018;173:442–8. http://dx.doi.org/10.1016/j.engstruct.2018.06.111, https://www.sciencedirect.com/science/article/pii/S0141029618306746.
[9] Faghidian SA, Elishakoff I. The tale of shear coefficients in Timoshenko–Ehrenfest beam theory: 130 years of progress. Meccanica 2023;58(1):97–108.
[10] Nie G, Zhong Z, Chen S. Analytical solution for a functionally graded beam with arbitrary graded material properties. Composites B 2013;44(1):274–82. http://dx.doi.org/10.1016/j.compositesb.2012.05.029, https://www.sciencedirect.com/science/article/pii/S1359836812003551.
[11] Vilar M, Hadjiloizi D, Masjedi PK, Weaver PM. Stress analysis of generally asymmetric non-prismatic beams subject to arbitrary loads. Eur J Mech A Solids 2021;90:104284. http://dx.doi.org/10.1016/j.euromechsol.2021.104284, https://www.sciencedirect.com/science/article/pii/S0997753821000668.
[12] Elishakoff I. Handbook on timoshenko-ehrenfest beam and uflyand-mindlin plate theories. World Scientific; 2020.
[13] Karabalis D, Beskos D. Static, dynamic and stability analysis of structures composed of tapered beams. Comput Struct 1983;16(6):731–48. http://dx.doi.org/10.1016/0045-7949(83)90064-0, https://www.sciencedirect.com/science/article/pii/0045794983900640.
[14] Eisenberger M. Explicit stiffness matrices for non-prismatic members. Comput Struct 1985;20(4):715–20. http://dx.doi.org/10.1016/0045-7949(85)90032-X, https://www.sciencedirect.com/science/article/pii/004579498590032X.
[15] Aristizabal-Ochoa JD. Tapered beam and column elements in unbraced frame structures. J Comput Civ Eng 1987;1(1):35–49. http://dx.doi.org/10.1061/(ASCE)0887-3801(1987)1:1(35).
[16] Eisenberger M. Exact solution for general variable cross-section members. Comput Struct 1991;41(4):765–72. http://dx.doi.org/10.1016/0045-7949(91)90186-P, https://www.sciencedirect.com/science/article/pii/004579499190186P.
[17] Murin J, Kutis V. 3D-beam element with continuous variation of the cross-sectional area. Comput Struct 2002;80(3):329–38. http://dx.doi.org/10.1016/S0045-7949(01)00173-0, https://www.sciencedirect.com/science/article/pii/S0045794901001730.
[18] Al-Gahtani HJ. Exact stiffnesses for tapered members. J Struct Eng 1996;122(10):1234–9. http://dx.doi.org/10.1061/(ASCE)0733-9445(1996)122:10(1234).
[19] Yao-Zhi L, Xian X, Fang W. Accurate stiffness matrix for nonprismatic members. J Struct Eng 2007;133(8):1168–75. http://dx.doi.org/10.1061/(ASCE)0733-9445(2007)133:8(1168).
[20] Failla G, Impollonia N. General finite element description for non-uniform and discontinuous beam elements. Arch Appl Mech 2012;82(1):43–67. http://dx.doi.org/10.1007/s00419-011-0538-8.
[21] Biondi B, Caddemi S, Marletta M. Exact static deflection of non-uniform Euler-Bernoulli beams with flexural stiffness singularities. Meccanica dei Materiali e delle Strutture 2010;1(3):24–43.
[22] Jones E, et al. The flexure of a non-uniform beam. Pacific J Math 1955;5(5):799–806.
[23] Romano F, Zingone G. Deflections of beams with varying rectangular cross section. J Eng Mech 1992;118(10):2128–34. http://dx.doi.org/10.1061/(ASCE)0733-9399(1992)118:10(2128).

[24] Romano F, Zingone G. Deflections of members with variable circular cross-section. Int J Mech Sci 1992;34(6):419–34. http://dx.doi.org/10.1016/0020-7403(92)90009-6, https://www.sciencedirect.com/science/article/pii/0020740392900096.

[25] Sankar B. An elasticity solution for functionally graded beams. Compos Sci Technol 2001;61(5):689–96. http://dx.doi.org/10.1016/S0266-3538(01)00007-0, https://www.sciencedirect.com/science/article/pii/S0266353801000070.

[26] Yang Q, Zheng B, Zhang K, Li J. Elastic solutions of a functionally graded cantilever beam with different modulus in tension and compression under bending loads. Appl Math Model 2014;38(4):1403–16. http://dx.doi.org/10.1016/j.apm.2013.08.021, https://www.sciencedirect.com/science/article/pii/S0307904X13005313.

[27] Eisenberger M. Stiffness matrices for non-prismatic members including transverse shear. Comput Struct 1991;40(4):831–5. http://dx.doi.org/10.1016/0045-7949(91)90312-A, https://www.sciencedirect.com/science/article/pii/004579499190312A.

[28] Tena-Colunga A. Stiffness formulation for nonprismatic beam elements. J Struct Eng 1996;122(12):1484–9. http://dx.doi.org/10.1061/(ASCE)0733-9445(1996)122:12(1484).

[29] Shooshtari A, Khajavi R. An efficient procedure to find shape functions and stiffness matrices of nonprismatic Euler–Bernoulli and Timoshenko beam elements. Eur J Mech A Solids 2010;29(5):826–36. http://dx.doi.org/10.1016/j.euromechsol.2010.04.003, https://www.sciencedirect.com/science/article/pii/S0997753810000586.

[30] Palacio-Betancur A, Aristizabal-Ochoa J Darío. Second-order stiffness matrix and loading vector of a tapered rectangular Timoshenko beam–column with semirigid connections. Structures 2018;15:211–23. http://dx.doi.org/10.1016/j.istruc.2018.07.002, https://www.sciencedirect.com/science/article/pii/S2352012418300663.

[31] Gendy OE, Sallam E, Mohamedien MA. Finite element formulation of Timoshenko tapered beam–column element for large displacement analysis based on the exact shape functions. Austral J Struct Eng 2022;23(3):269–88. http://dx.doi.org/10.1080/13287982.2022.2070958.

[32] Chockalingam SN, Pandurangan V, Nithyadharan M. [T]imoshenko beam formulation for in-plane behaviour of tapered monosymmetric i-beams: Analytical solution and exact stiffness matrix. Thin-Walled Struct 2021;162:107604. http://dx.doi.org/10.1016/j.tws.2021.107604, https://www.sciencedirect.com/science/article/pii/S0263823121001269.

[33] Romano F. Deflections of Timoshenko beam with varying cross-section. Int J Mech Sci 1996;38(8):1017–35. http://dx.doi.org/10.1016/0020-7403(95)00092-5, https://www.sciencedirect.com/science/article/pii/0020740395000925.

[34] Medwadowski SJ. Nonprismatic shear beams. J Struct Eng 1984;110(5):1067–82. http://dx.doi.org/10.1061/(ASCE)0733-9445(1984)110:5(1067).

[35] Lee S, Kuo Y. Static analysis of nonuniform Timoshenko beams. Comput Struct 1993;46(5):813–20. http://dx.doi.org/10.1016/0045-7949(93)90144-3, https://www.sciencedirect.com/science/article/pii/0045794993901443.

[36] Gupta AK. Vibration of tapered beams. J Struct Eng 1985;111(1):19–36.

[37] Banerjee JR, Williams FW. Exact Bernoulli–Euler dynamic stiffness matrix for a range of tapered beams. Internat J Numer Methods Engrg 1985;21(12):2289–302. http://dx.doi.org/10.1002/nme.1620211212, arXiv:https://onlinelibrary.wiley.com/doi/pdf/10.1002/nme.1620211212, https://onlinelibrary.wiley.com/doi/abs/10.1002/nme.1620211212.

[38] Klein L. Transverse vibrations of non-uniform beams. J Sound Vib 1974;37(4):491–505. http://dx.doi.org/10.1016/S0022-460X(74)80029-5, https://www.sciencedirect.com/science/article/pii/S0022460X74800295.

[39] Hsu J-C, Lai H-Y, Chen C. Free vibration of non-uniform Euler–Bernoulli beams with general elastically end constraints using adomian modified decomposition method. J Sound Vib 2008;318(4):965–81. http://dx.doi.org/10.1016/j.jsv.2008.05.010, https://www.sciencedirect.com/science/article/pii/S0022460X08004653.

[40] Çelik Ibrahim. Free vibration of non-uniform Euler–Bernoulli beam under various supporting conditions using Chebyshev wavelet collocation method. Appl Math Model 2018;54:268–80. http://dx.doi.org/10.1016/j.apm.2017.09.041, https://www.sciencedirect.com/science/article/pii/S0307904X17305942.

[41] Mahmoud M. Free vibrations of tapered and stepped, axially functionally graded beams with any number of attached masses. Eng Struct 2022;267:114696. http://dx.doi.org/10.1016/j.engstruct.2022.114696, https://www.sciencedirect.com/science/article/pii/S014102962200788X.

[42] Caliò I, Elishakoff I. Closed-form solutions for axially graded beam–columns. J Sound Vib 2005;280(3):1083–94. http://dx.doi.org/10.1016/j.jsv.2004.02.018, https://www.sciencedirect.com/science/article/pii/S0022460X04005383.

[43] Attarnejad R, Jandaghi Semnani S, Shahba A. Basic displacement functions for free vibration analysis of non-prismatic Timoshenko beams. Finite Elem Anal Des 2010;46(10):916–29. http://dx.doi.org/10.1016/j.finel.2010.06.005, https://www.sciencedirect.com/science/article/pii/S0168874X10000910.

[44] Yuan J, Mu Z, Elishakoff I. Novel modification to the timoshenko–ehrenfest theory for inhomogeneous and nonuniform beams. AIAA J 2020;58(2):939–48. http://dx.doi.org/10.2514/1.J056885.

[45] Shakya NK, Padhee SS. Asymptotic analysis of timoshenko-like orthotropic beam with elliptical cross-section. Eur J Mech A Solids 2023;102:105100. http://dx.doi.org/10.1016/j.euromechsol.2023.105100, https://www.sciencedirect.com/science/article/pii/S0997753823001924.

[46] Molina-Villegas JC, Ballesteros Ortega JE, Martínez G Martínez. Closed-form solution for non-uniform Euler–Bernoulli beams and frames. Eng Struct 2023;292:116381. http://dx.doi.org/10.1016/j.engstruct.2023.116381, https://www.sciencedirect.com/science/article/pii/S0141029623007964.

[47] Williams FW, Kennedy D, Djoudi MS. Exact determinant for infinite order FEM representation of a timoshenko beam–column via improved transcendental member stiffness matrices. Internat J Numer Methods Engrg 2004;59(10):1355–71. http://dx.doi.org/10.1002/nme.919, arXiv:https://onlinelibrary.wiley.com/doi/pdf/10.1002/nme.919, https://onlinelibrary.wiley.com/doi/abs/10.1002/nme.919.

[48] Adhikari S. Exact transcendental stiffness matrices of general beam–columns embedded in elastic mediums. Comput Struct 2021;255:106617. http://dx.doi.org/10.1016/j.compstruc.2021.106617, https://www.sciencedirect.com/science/article/pii/S0045794921001395.

[49] Molina-Villegas JC, Diaz Giraldo HN, Acosta Ochoa AF. Analytical formulation of the stiffness method for 2D reticular structures using Green functions. Revista Internacional de Métodos Numéricos para Cálculo y Diseño en Ingeniería 2020;36(3). http://dx.doi.org/10.23967/j.rimni.2020.09.004.

[50] Molina-Villegas JC. Análisis estructural - métodos clásicos y matriciales. ECOE Ediciones 2021.

[51] Molina-Villegas JC, Ballesteros Ortega JE, Ruiz Cardona D. Formulation of the green's functions stiffness method for Euler–Bernoulli beams on elastic winkler foundation with semi-rigid connections. Eng Struct 2022;266:114616. http://dx.doi.org/10.1016/j.engstruct.2022.114616, https://www.sciencedirect.com/science/article/pii/S0141029622007155.

[52] Molina-Villegas JC, Ballesteros Ortega JE. Closed-form solution of Timoshenko frames with semi-rigid connections. Structures 2023;48:212–25. http://dx.doi.org/10.1016/j.istruc.2022.12.082, https://www.sciencedirect.com/science/article/pii/S235201242201270X.

[53] Molina-Villegas JC, Ballesteros Ortega JE. Closed-form solution of Timoshenko frames using the Green's function stiffness method. Int J Solids Struct 2023;269:112180. http://dx.doi.org/10.1016/j.ijsolstr.2023.112180, https://www.sciencedirect.com/science/article/pii/S002076832300077X.

[54] Molina-Villegas JC, Ballesteros Ortega JE. Closed-form solution of Euler–Bernoulli frames in the frequency domain. Eng Anal Bound Elem 2023;155:682–95. http://dx.doi.org/10.1016/j.enganabound.2023.06.027, https://www.sciencedirect.com/science/article/pii/S0955799723003430.

[55] Ballesteros Ortega JE, Posso C, Molina-Villegas JC. Analytical frequency-domain solution for Euler-Bernoulli frames with semi-rigid connections. Forces Mech. 2024;14:100252. http://dx.doi.org/10.1016/j.finmec.2023.100252, https://www.sciencedirect.com/science/article/pii/S2666359723000872.

[56] Faghidian SA, Elishakoff I. The tale of shear coefficients in Timoshenko–Ehrenfest beam theory: 130 years of progress. Meccanica 2023;58(1):97–108.

[57] Reddy JN. Introduction to the finite element method. McGraw-Hill Education; 2019.

[58] Huang Y, Ouyang Z-Y. Exact solution for bending analysis of two-directional functionally graded Timoshenko beams. Arch Appl Mech 2020;90(5):1005–23. http://dx.doi.org/10.1007/s00419-019-01655-5.

[59] Tudjono S, Han A, Nguyen D-K, Kiryu S, Gan BS. Exact shape functions for timoshenko beam element. IOSR J Comput Eng 2017;19(03):12–20.

[60] Bathe K-J. Finite element procedures. Klaus-Jurgen Bathe; 2006.

[61] Kaneko T. On Timoshenko's correction for shear in vibrating beams. J Phys D: Appl Phys 1975;8(16):1927–36. http://dx.doi.org/10.1088/0022-3727/8/16/003.

[62] Rosinger HE, Ritchie IG. On timoshenko's correction for shear in vibrating isotropic beams. J Phys D: Appl Phys 1977;10(11):1461–6. http://dx.doi.org/10.1088/0022-3727/10/11/009.

[63] McKenna F, Scott MH, Fenves GL. Nonlinear finite-element analysis software architecture using object composition. J Comput Civ Eng 2010;24(1):95–107. http://dx.doi.org/10.1061/(ASCE)CP.1943-5487.0000002.

[64] Rakowski J. The interpretation of the shear locking in beam elements. Comput Struct 1990;37(5):769–76. http://dx.doi.org/10.1016/0045-7949(90)90106-C, https://www.sciencedirect.com/science/article/pii/004579499090106C.